Bull. Chem. Soc. Ethiop. **2024**, 38(6), 1791-1801.
DOI: https://dx.doi.org/10.4314/bcse.v38i6.22

ISSN 1011-3924
Printed in Ethiopia
Online ISSN 1726-801X

PREPARATION AND CHARACTERIZATIONS OF METAL-BASED COMPLEXES DERIVED FROM THE REACTION OF TRIZMA BASE WITH Mg(II), Ca(II), AND Ba(II) IONS

Abdel Majid A. Adam[1*], Moamen S. Refat[1], Amnah Mohammed Alsuhaibani[2] and Mohamed Y. El-Sayed[3]

[1]Department of Chemistry, College of Science, Taif University, P.O. Box 11099, Taif 21944, Saudi Arabia
[2]Department of Physical Sport Science, College of Sport Sciences & Physical Activity, Princess Nourah bint Abdulrahman University, P.O. Box 84428, Riyadh 11671, Saudi Arabia
[3]Department of Chemistry, College of Science, Jouf University, Sakaka 2014, Saudi Arabia

(Received July 18, 2024; Revised August 30, 2024; Accepted September 3, 2024)

ABSTRACT. Trizma base is a small organic compound that possesses one amino group (-NH_2) and three hydroxyl groups (-OH). Three products of trizma base as a ligand were prepared from the reaction of Mg(II), Ca(II), and Ba(II) ions with the ligand at a temperature of 65 °C and stoichiometry of 1:1 (ligand to metal ion). The trizma ligand was referred to as Tris, and its complexes with Mg(II), Ca(II), and Ba(II) ions were referred to as Product 1, Product 2, and Product 3, respectively. After the preparation of the products, they were characterized by several analytical methods, including spectroscopies [Fourier-transform infrared (FT-IR) and ultraviolet/visible (UV-visible)], thermogravimetry (TG), elemental analyses, X-ray diffraction (XRD), and scanning electron microscope with environmental mode (ESEM). Analytical results suggested that Tris ligand captured the investigated metal ions using the amino group (-NH_2) and one hydroxyl group (-OH) forming complexes with general composition of $[MgTris(H_2O)_4]\cdot Cl_2\cdot 2H_2O$ (Product 1), $[CaTris(H_2O)_4]\cdot Cl_2\cdot 2H_2O$ (Product 2), $[BaTris(H_2O)_4]\cdot Cl_2\cdot H_2O$ (Product 3). The corresponding gross formulas for these products were $C_4H_{23}NO_9MgCl_2$ (324.34), $C_4H_{23}NO_9CaCl_2$ (340.11), and $C_4H_{21}NO_8BaCl_2$ (419.37 g/mol), respectively. SEM micrographs captured at high levels of magnification (×100,000) clearly illustrate variations in the morphology of products 1, 2, and 3.

KEY WORDS: Trizma base, Spectral analysis, Thermogravimetry, SEM micrographs

INTRODUCTION

The reaction of metal ions with organic molecules generates an important and interesting class of chemical compounds known as metal-based complexes. The importance of this class of compounds increases when the metal ions react with bioactive molecules such as drugs. This special type of metal-based complexes is known as metal-based drugs or metallodrugs. The coordination chemistry of metal-based complexes and metallodrugs received considerable interest from researchers due to the wide applications of these complexes in chemistry, biology, and pharmacology fields [1-12]. Numerous metal-based -drugs and -complexes exhibit potential antibacterial, antiviral, and anticancer properties. This enables them to be used as therapeutic and chemotherapeutics agents for several human diseases such as carcinomas, infection control, inflammation, cancer, neurological disorders, and diabetes [13-17]. Drug resistance and adverse side effects of several metal-based drugs, and the occurrence of new diseases such as coronavirus disease (COVID-19), which was caused by a novel coronavirus named SARS-CoV-2, motivate researchers to investigate new chemical reactions of metal ions with different kinds of molecules to design and development of more biologically active metal-based complexes. Trizma base is a small organic compound that possesses one amino group (-NH_2) and three hydroxyl groups (-OH) (Figure 1). This compound, which exists as a white crystalline powder, has an IUPAC name: 2-amino-2-(hydroxymethyl)-1,3-propanediol. Trizma base has several synonyms, such as

*Corresponding authors. E-mail: majidadam@tu.edu.sa

Trometamol, Trisaminol, Tris buffer, and Tris base. Trizma base has wide applications in medicine, biochemistry, biology, and physiology [18-20]. Clinically, it is used to reverse acidosis, and biochemically, it is used as a buffer for several biochemical processes [21, 22].

The aim of this work was to synthesize and characterize three metal complexes of Tris ligand containing Mg(II), Ca(II), and Ba(II) ions. This aim was achieved in two steps. First, we synthesized Product 1, Product 2, and Product 3 from the reaction of the Tris ligand with Mg(II), Ca(II), and Ba(II) ions, respectively. The reaction occurred at a temperature of 65 °C and stoichiometry of 1:1 (ligand to metal ion). Then, we investigated the mode of interaction between Tris ligand and the investigated metal ions based on the elemental and spectral data collected from CHN elemental analyses results, Fourier-transform infrared (FT-IR), and ultraviolet/visible (UV-visible) spectroscopies. Finally, we observed the thermal decomposition behavior, phase purity, and outer surface morphology of the obtained products by thermogravimetry (TG), X-ray diffraction (XRD), and scanning transmission electron microscopy (SEM) techniques.

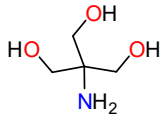

Figure 1. Molecular structure of Trizma.

EXPERIMENTAL

Materials

Analytical grade trizma base [$NH_2C(CH_2OH)_3$; 121.14 g/mol] was purchased from BDH Chemicals (UK) at the highest purity (≥ 99.9%). Fluka Company (Seelze, Germany) provided $MgCl_2$ (95.21 g/mol), $CaCl_2$ (110.98 g/mol), and $BaCl_2{\cdot}2H_2O$ (244.26 g/mol) in analytical grade at the highest purity (99.9%). Deionized water obtained using a Milli-Q system and HPLC-grade methanol (MeOH) from Merck Chemical Company (KGaA, Germany) are solvents used for the preparation.

Preparation

Metal-based complexes of Tris ligand with Mg(II), Ca(II), and Ba(II) ions were prepared via three steps: (i) Dissolving: Tris ligand was dissolved in methanol (2.0 mmol; 25 mL), where each of the metal chloride was dissolved in deionized water (2.0 mmol; 25 mL). (ii) Reaction: Methanolic solution of Tris was mixed with the aqueous solution of the metal chloride. The temperature of the mixture was adjusted at 65 °C. The mixture was stirred on a multi-position hotplate stirrer for 20 min. (iii) Separation and purification: The mixture solution was reduced to one-half by evaporating on a water bath. The formed precipitates were left overnight at room temperature to ensure the complete of the precipitation. The precipitates were filtered off and washed several times with methanol. The product was re-crystallized from methanol, filtered off, and finally dried in vacuum for 72 h. Complexes of Mg(II), Ca(II), and Ba(II) with Tris were termed as Product 1, Product 2, and Product 3, respectively.

Analytical methods

The UV-Visible, FT-IR, and XRD spectra of the synthesized metal-based complexes of Tris ligand were collected using Perkin-Elmer Lambda 25 UV/Vis spectrophotometer, Shimadzu

Fourier-transform infrared spectrophotometer, and X'Pert Philips X-ray diffractometer, respectively. Shimadzu TG/DTG-50H thermal analyzer was used to collect the thermograms of the complexes. Perkin-Elmer 2400 series II CHN elemental analyzer was used to measure the elemental composition of the complexes. Thermo Fisher Scientific high resolution Scanning Electron Microscope with environmental mode (Quattro ESEM) was used to capture the SEM micrographs.

RESULTS AND DISCUSSION

C, H, N elemental analyses and UV-visible spectra

Perkin-Elmer CHN elemental analyzer was used to measure the elemental composition of C%, H%, and N% in the synthesized products. The metal and water contents in (%) in these products were determined gravimetrically. Elemental results for Product 1: calc. (found) for C, 14.80% (14.58); H, 7.09% (7.20); N, 4.32% (4.47); Mg, 7.49% (7.23); Water, 33.30% (33.05). Elemental results for Product 2: calc. (found) for C, 14.11% (13.96); H, 6.76% (6.65); N, 4.12% (4.35); Ca, 11.78% (12.00); Water, 31.75% (31.90). Elemental results for Product 3: calc. (found) for C, 11.44% (11.60); H, 5.00% (4.83); N, 3.34% (3.57); Ba, 32.75% (32.56); Water, 21.46% (21.68). Based on the elemental composition results, the suggested general compositions of Product 1, Product 2, and Product 4 were $[MgTris(H_2O)_4]\cdot Cl_2\cdot 2H_2O$, $[CaTris(H_2O)_4]\cdot Cl_2\cdot 2H_2O$, and $[BaTris(H_2O)_4]\cdot Cl_2\cdot H_2O$, respectively. The corresponding gross formulas were $C_4H_{23}NO_9MgCl_2$ (324.34), $C_4H_{23}NO_9CaCl_2$ (340.11), $C_4H_{21}NO_8BaCl_2$ (419.37 g/mol), respectively. These gross formulas are indicative of a 1:1 metal-to-ligand stoichiometry.

Figure 2 contains the UV-visible spectra of Products 1, 2, and 3. All products absorbed only in the UV region. Product 1 gives two absorption bands in the range from 200 to 300 nm. A very strong, intense, and narrow absorption band at 210 nm. A medium-intensity, broad absorption band located at 232 nm. The broad band has a shoulder band at 258 nm. Product 2 behaved similarly to Product 1. It gives two absorption bands, an intense, and narrow absorption band at 225 nm, and a medium-intensity, broad absorption band at 246 nm. The broad band also has a shoulder band at 258 nm. The UV-Visible spectrum of Product 3 exhibits a single very strong, intense absorption band at 230 nm. This band also has shoulder band at 258 nm. The maximum wavelength (λ_{max}) of the intense absorption band was shifted from 210 nm in Product 1, to 225 nm in product 2, to 230 nm in Product 3. All these electronic absorptions can be assigned to the $\pi\rightarrow\pi^*$ transitions.

FT-IR spectra

The free Tris ligand and its products with Mg(II), Ca(II), and Ba(II) ions were scanned by a FTIR spectrophotometer collected from 400 to 4000 cm^{-1}. Table 1 lists the FTIR frequencies (cm^{-1}) of free Tris ligand and the synthesized products. The free Tris ligand has several different functional groups: O–H, $–NH_2$, C–O, and C–N. The FTIR spectrum of free Tris ligand contains several distinguished absorption bands [23]. The amino ($–NH_2$) group generated several stretching and bending vibrations, namely $\nu(NH_2)$, $\delta_{sciss}(NH_2)$, $\delta_{wag}(NH_2)$, and $\delta_{rock}(NH_2)$, which appeared at 3195, 1545, 1329, and 645 cm^{-1}, respectively. The hydroxyl (O–H) group generated several stretching and bending vibrations, namely ν(O–H), δ_{def}(O–H), δ(O–H) in-plane bending, and δ(O–H) out-of-plane bending, which appeared at 3351, 1400, 924, and 778 cm^{-1}, respectively. The bands at 1462, 1372, 1292 and 1039 cm^{-1} resulted from the vibrations of $\delta_{sciss}(CH_2)$, δ_{def}(C–H), ν(C–N), and ν(C–O), respectively. The complexation between the Tris ligand with the investigated metal ions decreases the broadening and the intensity of the FTIR bands resulted from the ν(O–H) and ($–NH_2$) vibrations. The frequency of the $\nu(NH_2)$ vibrations was shifted from 3195 cm^{-1} in the free Tris ligand to 3287 cm^{-1} in the Product 1, to 3282 cm^{-1} in the Product 2, and to 3288

cm^{-1} in the Product 3. The frequency of the ν(O–H) vibrations was shifted from 3351 cm^{-1} in the free Tris ligand to 3320 cm^{-1} in the Product 1, to 3323 cm^{-1} in the Product 2, and to 3327 cm^{-1} in the Product 3. Also, after the complexation process, the bands attributed to the $\delta_{sciss}(NH_2)$ and δ_{def}(O–H) vibrations were moved to higher frequencies. The band of $\delta_{sciss}(NH_2)$ occurs near 1545 cm^{-1} in the free Tris ligand was shifted to 1585, 1588, and 1586 cm^{-1} in Product 1, Product 2, and Product 3, respectively. The band of δ_{def}(O–H) occurs near 1400 cm^{-1} in the free Tris ligand was shifted to 1430, 1445, and 1460 cm^{-1} in Product 1, Product 2, and Product 3, respectively. All these shifts suggested that O–H and $-NH_2$ groups participate in the complexation process. Absorption bands originated from the four angular deformation motion of coordinated water molecules were observed in the FTIR spectra of the products around 580-582, 675-670, 850-847, and 1638-1634, attributed to the $\delta_{twist}(H_2O)$, $\delta_{wag}(H_2O)$, $\delta_{rock}(H_2O)$, and $\delta_{bend}(H_2O)$, respectively [24]. The ν(M-O) vibrational bands have been registered in the region 525-560 cm^{-1}.

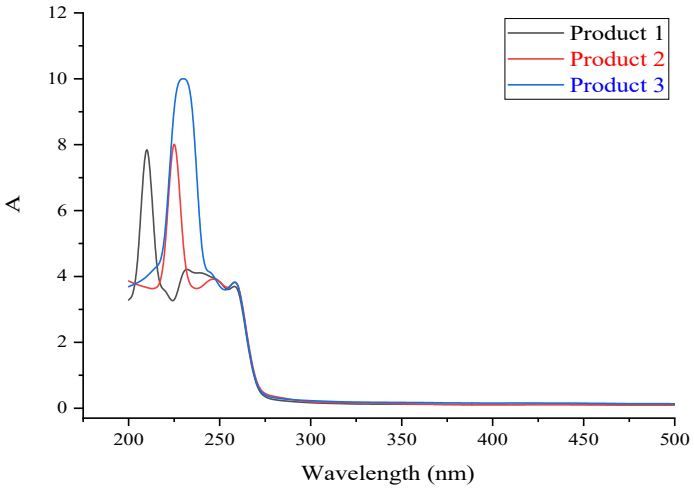

Figure 2. UV-visible spectra of the synthesized Product 1, Product 2, and Product 3.

XRD data

The phase purity and framework structure of Products 1, 2, and 3 were checked by performing the XRD measurements in the 2θ range of 10-80°. Table 2 lists the XRD spectral data of the strongest three peaks for the synthesized products obtained from their XRD diffractograms. Product 1 had one very strong line at Bragg diffraction angle 2θ 22.0612°, one medium-strong line at 11.2600°, and one medium line at 40.8333°. A group of medium-to-weak intensity lines were observed in the XRD spectrum of product 1 in the range 2θ 15°-60°. Product 2 had three very strong diffraction lines at Bragg's angle 2θ 44.2003°, 21.5684°, and 20.6962°. The absence of a single, sharp strong, and intense line in the XRD profile of Product 2 suggests that this product mainly possess an amorphous structure. Only one very strong, sharp, and intense diffraction line was observed for Product 3 at 2θ 20.2978. The other lines in this product were medium or weak intensity. The XRD profile of product 3 suggests that this product had a well-crystallized and well-defined morphology. Product 3 had higher degree of crystallinty than other products. The inter-planar spacing between the atoms (*d*-spacing) values in (Å) of the strongest line detected in the products' XRD diffractograms were 4.02596, 2.04744, and 4.37157 for products 1, 2, and 3,

respectively. Values of the full-width at half-maximum of the strongest line (FWHM) in (deg) for the products 1, 2, and 3 were 0.47870, 0.49880, and 0.55710, respectively.

Table 1. The FTIR frequencies (cm^{-1}) and their tentative vibrational modes for the free Tris ligand, Product 1, Product 2, and Product 3.

Wavelength (cm^{-1})				Mode of vibration
Free Tris ligand	Product 1	Product 2	Product 3	
3351	3320	3323	3327	ν(O–H)
3195	3287	3282	3288	$\nu(NH_2)$
2938	2938	2930	2940	$\nu_{as}(CH_2)$
2875	2870, 2844	2877, 2848	2863, 2845	$\nu_s(CH_2)$
-	1634	1638	1634	$\delta_b(H_2O)$
1545	1585	1588	1586	$\delta_{sciss}(NH_2)$
1462	1466	1465	1460	$\delta_{sciss}(CH_2)$
1400	1430	1445	1460	δ_{def}(O–H)
1372	1396	1395	1397	δ_{def}(C–H)
1329	1315	1315	1340	$\delta_{wag}(NH_2)$
1292	1290	1290	1287	ν(C–N)
1215	1210	1216	1212	ν(C–C)
1150	1175	1173	1170	$\delta_{rock}(CH_2)$
1136	1163	1159	1157	$\delta_{twist}(NH_2)$
1039	1028	1040	1019	ν(C–O)
924	927	934	919	δ(O–H) in-plane bending
900	895	897	895	δ_{def}(C–H)
780	872	873	862	$\delta_{wag}(CH_2)$
-	847	848	850	$\delta_{rock}(H_2O)$
778	784	788	785	δ(O–H) out-of-plane bending
-	672	675	670	$\delta_{wag}(H_2O)$
645	652	651	650	$\delta_{rock}(NH_2)$
600	602	603	600	$\delta_{rock}(CH_2)$
-	580	583	582	$\delta_{twist}(H_2O)$
-	560, 524	551, 528	563, 525	ν(M–O)
441	466	461	468	$\delta_{twist}(CH_2)$

Table 2. The XRD spectral data of the strongest three peaks for the synthesized products.

Product	XRD data					
	Peak no.	2θ (deg)	*d*-spacing value; (Å)	Intensity (I/I1)	FWHM (deg)	Intensity (counts)
Product 1	4	22.0612	4.02596	100	0.47870	1131
	1	11.2600	7.85187	72	0.52210	811
	13	40.8333	2.20815	48	0.28920	548
Product 2	24	44.2003	2.04744	100	0.49880	254
	6	21.5684	4.11682	98	0.52210	249
	5	20.6962	4.28830	84	0.54030	214
Product 3	3	20.2978	4.37157	100	0.55710	1865
	9	30.7712	2.90335	45	0.70810	836
	18	43.7060	2.06944	29	0.83260	549

Surface morphologies of Tris complexes

Figures 3, 4, and 5 displays the SEM micrographs of products 1, 2, and 3, respectively, captured at different levels of magnification ranging from x5000 to x100,000 at accelerating voltage of 20 kV. Four micrographs were provided for each product, and these micrographs clearly illustrate variations in the morphology of the products 1, 2, and 3. These SEM micrographs gave information on particle shape, surface topology and microstructure of the synthesized products. Product 1 comprised big agglomerates. Upon closer examination in the highly magnified micrographs (×50,000 and ×100,000), the surfaces of these aggregates are very smooth, and free from cracks and gaps, however small granules were observed on the surface. Product 2 consisted of particles with diverse features, irregular shapes, and sizes. Product 3 possessed stone-like shaped structures. These particles had different shapes and sizes.

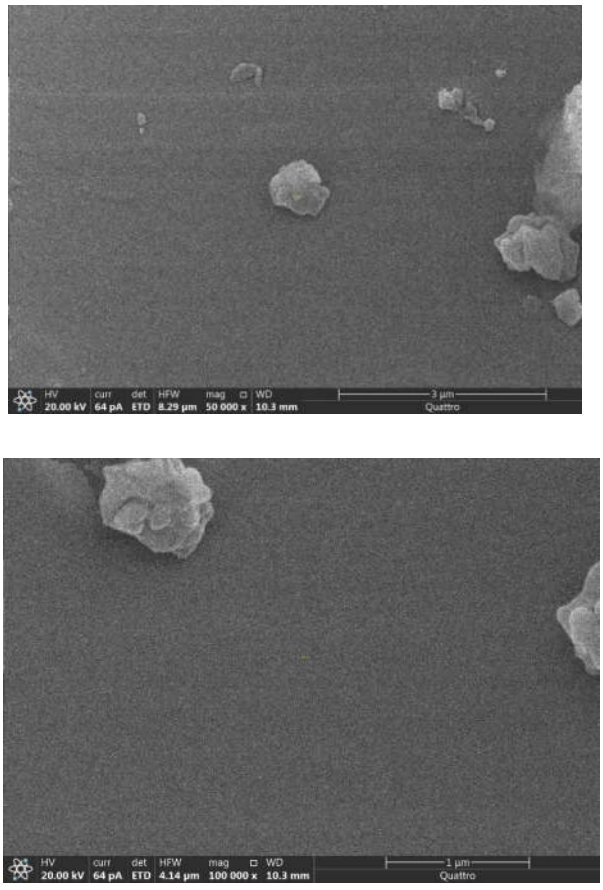

Figure 3. SEM micrographs of Product 1.

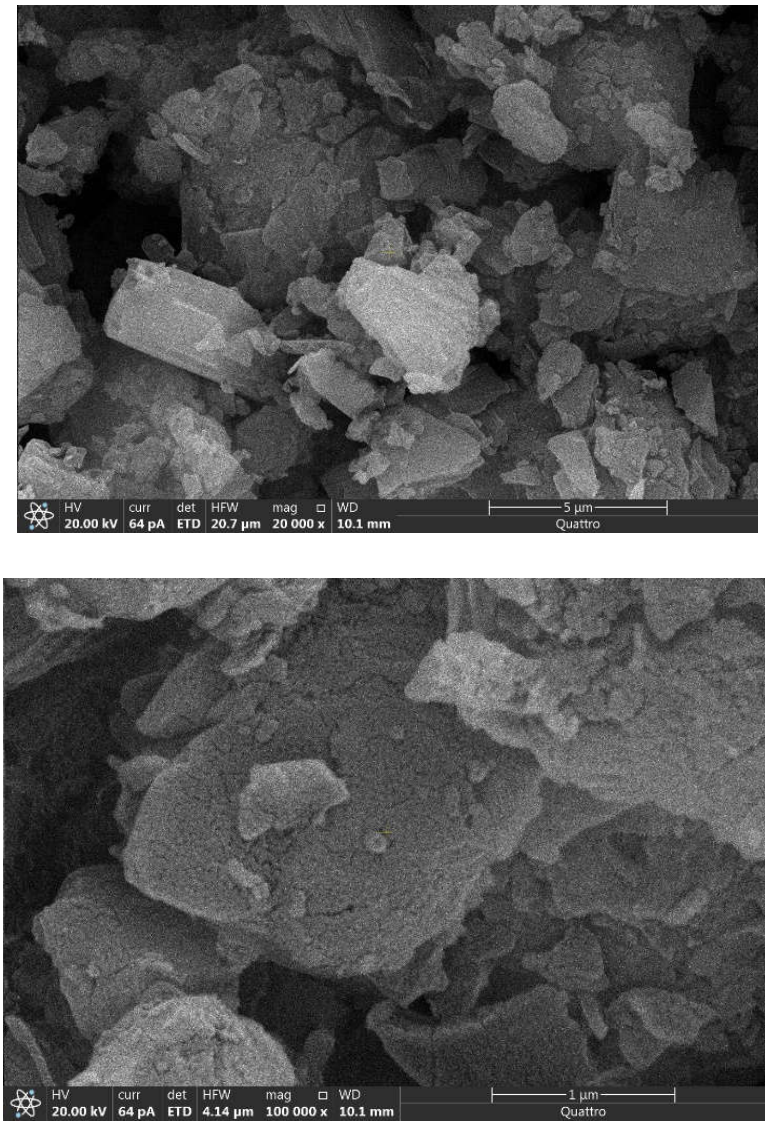

Figure 4. SEM micrographs of Product 2.

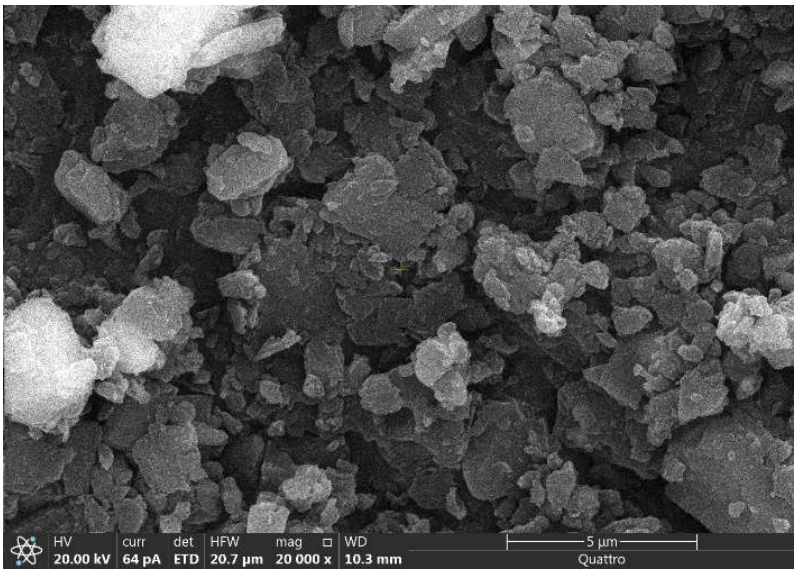

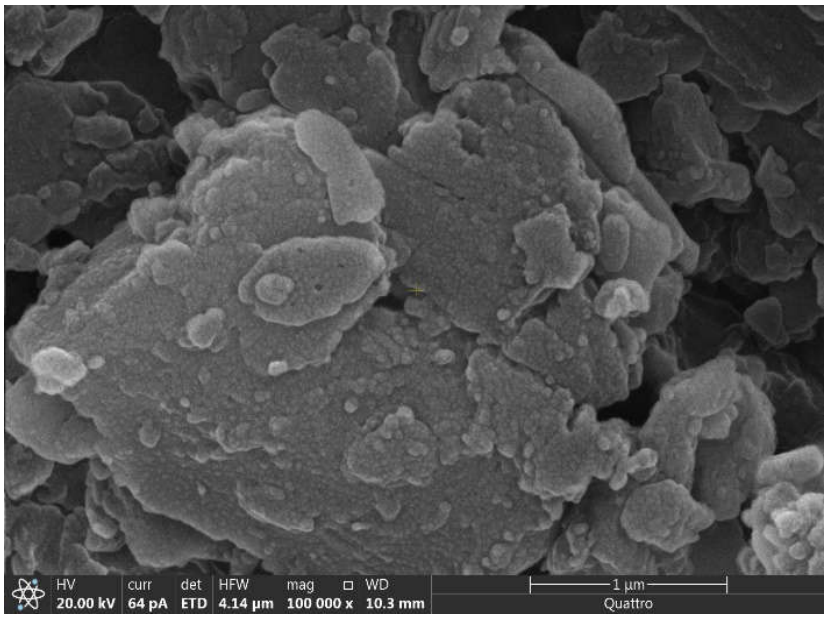

Figure 5. SEM micrographs of Product 3.

Thermal stability of Tris complexes

The thermograms of Product 1, Product 2, and Product 3 are illustrated in Figure 6. These thermograms indicated that Product 1, product 2, and Product 3 were thermally stable up to 100, 90, and 75 °C, respectively. This revealed that the synthesized products are stable at room temperature and can be stored without any thermal decomposition. Products 2 and 3 were decomposed in two-stage degradation steps in temperature range of 90-300 and 300-600 °C for Product 2, and in temperature range of 75-175 and 175-600 °C for Product 3. While Product 3 was decomposed in three-stage degradation steps in temperature range of 100-300, 300-415, and 415-600 °C. The degradations of Product 2 and Product 3 were almost completed with leaving $CaCO_3$ and $BaCO_3$, respectively. The degradation of Product 1 was almost complete with leaving MgO. The three decomposition steps of Product 1 were corresponded to weight losses of 33.06% (cal. 33.30%), 36.15% (cal. 36.04%), and 10.42% (cal. 10.79%). The two decomposition steps of Product 2 were corresponded to weight losses of 52.23% (cal. 52.60%), and 23.47% (cal. 23.81%). The two decomposition steps of Product 3 were corresponded to weight losses of 21.20% (cal. 21.46%), and 36.00% (cal. 36.22%).

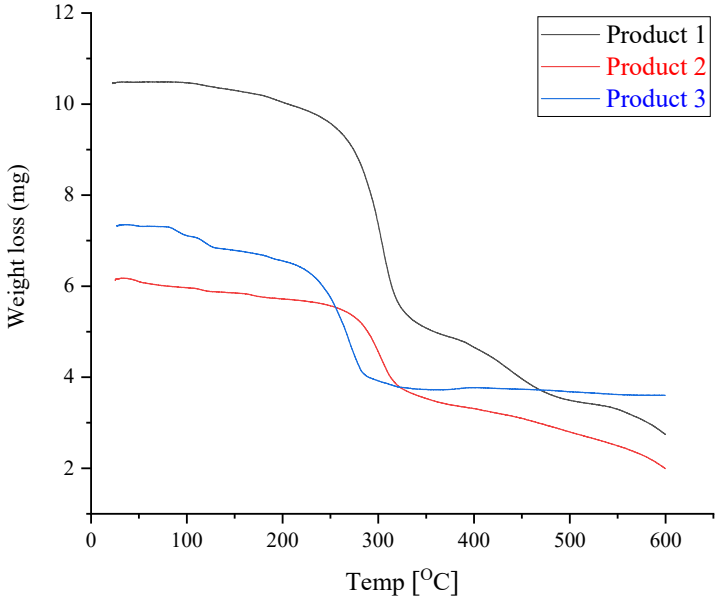

Figure 6. TG curves of the synthesized products.

CONCLUSION

The chemical reaction between Mg(II), Ca(II), and Ba(II) metal ions with the trizma base as a ligand at a stoichiometry of 2:1 (Tris to metal ion) at 65 °C generated thermally stable metal-based complexes. The generated products were termed as Product 1 [Mg(II)], product 2 [Ca(II)], and Product 3 [Ba(II)]. Ultraviolet/visible (UV-Visible), Fourier-transform infrared (FT-IR), thermogravimetry (TG), and elemental analysis data suggested that Tris ligand captured the investigated metal ions using the amino group ($-NH_2$) and one hydroxyl group (-OH) forming complexes. The obtained general composition of the synthesized products were

$[MgTris(H_2O)_4]\cdot Cl_2\cdot 2H_2O$ for Product 1, $[CaTris(H_2O)_4]\cdot Cl_2\cdot 2H_2O$ for Product 2, and $[BaTris(H_2O)_4]\cdot Cl_2\cdot H_2O$ for Product 3. ESEM micrographs captured at high levels of magnification (×100,000) clearly illustrate variations in the morphology of products 1, 2, and 3.

ACKNOWLEDGMENT

The authors extend their appreciation to Taif University, Saudi Arabia, for supporting this work through project number (TU-DSPP-2024-78).

FUNDING

This research was funded by Taif University, Saudi Arabia, Project No. (TU-DSPP-2024-78).

REFERENCES

1. El-Habeeb, A.A.; Refat, M.S. Synthesis, spectroscopic characterizations and biological studies on gold(III), ruthenium(III) and iridium(III) complexes of trimethoprim antibiotic drug. *Bull. Chem. Soc. Ethiop.* **2024**, 38, 701-714.
2. Alsuhaibani, A.M.; Adam, A.M.A.; Refat, M.S.; Kobeasy, M.I.; Bakare, S.B.; Bushara, E.S. Spectroscopic, thermal, and anticancer investigations of new cobalt(II) and nickel(II) triazine complexes. *Bull. Chem. Soc. Ethiop.* **2023**, 37, 1151-1162.
3. Younes, A.A.O.; Refat, M.S.; Saad, H.A.; Adam, A.M.A.; Alzoghibi, O.M.; Alsulaim, G.M.; Alsuhaibani, A.M. Complexation of some alkaline earth metals with bidentate uracil ligand: Synthesis, spectroscopic and antimicrobial analysis. *Bull. Chem. Soc. Ethiop.* **2023**, 37, 945-957.
4. Alkathiri, A.A.; Atta, A.A.; Refat, M.S.; Altalhi, T.A.; Shakya, S.; Alsawat, M.; Adam, A.M.A.; Mersal, G.A.M.; Hassanien, A.M. Preparation, spectroscopic, cyclic voltammetry and DFT/TD-DFT studies on fluorescein charge transfer complex for photonic applications. *Bull. Chem. Soc. Ethiop.* **2023**, 37, 515-532.
5. Adam, A.M.A.; Refat, M.S.; Gaber, A.; Grabchev, I. Complexation of alkaline earth metals Mg^{2+}, Ca^{2+}, Sr^{2+} and Ba^{2+} with adrenaline hormone: Synthesis, spectroscopic and antimicrobial analysis. *Bull. Chem. Soc. Ethiop.* **2023**, 37, 357-372.
6. Al-Hazmi, G.H.; Adam, A.M.A.; El-Desouky, M.G.; El-Bindary, A.A.; Alsuhaibani, A.M.; Refat, M.S. Efficient adsorption of Rhodamine B using a composite of Fe3O4@zif-8: Synthesis, characterization, modeling analysis, statistical physics and mechanism of interaction. *Bull. Chem. Soc. Ethiop.* **2023**, 37, 211-229.
7. Alsuhaibani, A.M.; Adam, A.M.A.; Refat, M.S. Four new tin(II), uranyl(II), vanadyl(II), and zirconyl(II) alloxan biomolecule complexes: synthesis, spectroscopic and thermal characterizations. *Bull. Chem. Soc. Ethiop.* **2022**, 36, 373-385.
8. Al-Hazmi, G.H.; Alibrahim, K.A.; Refat, M.S.; Ibrahim, O.B.; Adam, A.M.A.; Shakya, S. A new simple route for synthesis of cadmium(II), zinc(II), cobalt(II), and manganese(II) carbonates using urea as a cheap precursor and theoretical investigation. *Bull. Chem. Soc. Ethiop.* **2022**, 36, 363-372.
9. Alsuhaibani, A.M.; Refat, M.S.; Adam, A.M.A.; Kobeasy, M.I.; Kumar, D.N.; Shakya, S. synthesis, spectroscopic characterizations and DFT studies on the metal complexes of azathioprine immunosuppressive drug. *Bull. Chem. Soc. Ethiop.* **2022**, 36, 73-84.
10. El-Sayed, M.Y.; Refat, M.S.; Altalhi, T.; Eldaroti, H.H.; Alam, K. Preparation, spectroscopic, thermal and molecular docking studies of covid-19 protease on the manganese(II), iron(III), chromium(III) and cobalt(II) creatinine complexes. *Bull. Chem. Soc. Ethiop.* **2021**, 35, 399-412.

11. Alosaimi, A.M.; Saad, H.A.; Al-Hazmi, G.H.; Refat, M.S. In situ acetonitrile/water mixed solvents: An ecofriendly synthesis and structure Explanations of Cu(II), Co(II), and Ni(II) complexes of thioxoimidazolidine. *Bull. Chem. Soc. Ethiop.* **2021**, 35, 351-364.
12. Refat, M.S.; Altalhi, T.A.; Al-Hazmi, G.H.; Al-Humaidi, J.Y. Synthesis, characterization, thermal analysis and biological study of new thiophene derivative containing *o*-aminobenzoic acid ligand and its Mn(II), Cu(II) and Co(II) metal complexes. *Bull. Chem. Soc. Ethiop.* **2021**, 35, 129-140.
13. Tella, A.C.; Obaleye, J.A.; Olawale, M.D.; Ngororabanga, J.M.V.; Ogunlaja, A.S.; Bourned, S.A. Synthesis, crystal structure, and density functional theory study of a zinc(II) complex containing terpyridine and pyridine-2,6-dicarboxylic acid ligands: Analysis of the interactions with amoxicillin. *C.R. Chimie* **2019**, 22, 3-12.
14. Eichhorn, G.L.; Marzilli, L.G. *Advances in Inorganic Biochemistry Models in Inorganic Chemistry*, PTR Prentice-Hall, Inc.: New Jersey; **1994**.
15. Hughes, M.N. *The Inorganic Chemistry of Biological Processes*, 2nd ed., Wiley: Chichester, England; **1984**.
16. Alessio, E. *Bioinorganic Medicinal Chemistry*, Wiley-VCH Verlag GmbH:New York; **2011**.
17. Netalkar, P.P.; Netalkar, S.P.; Revankar, V.K. Transition metal complexes of thiosemicarbazone: Synthesis, structures and invitro antimicrobial studies. *Polyhedron* **2015**, 100, 215-222.
18. Bubb, W.A.; Berthon, H.A.; Kuchel, P.W. Tris Buffer reactivity with low-molecular-weight aldehydes: NMR characterization of the reactions of glyceraldehyde-3-phosphate. *Bioorg. Chem.* **1995**, 23, 119-130.
19. Brignac, P.J.; Mo, C. Formation constants and metal-to-ligand ratios for tris(hydroxymethyl)aminomethane-metal complexes. *Anal. Chem.* **1975**, 47, 1465-1466.
20. Hayashi, N.; Kinemuchi, H.; Kamijo, K. Effect of tris (hydroxymethyl) aminomethane on amine oxidase activity in dog brain, liver and serum and in human placenta. *Jap. J. Pharmacol.* **1981**, 31, 737-746.
21. Murakami, S.; Sudo, Y.; Miyano, K.; Nishimura, H.; Matoba, M.; Shiraishi, S.; Konno, H.; Uezono, Y. Tris-hydroxymethyl-aminomethane enhances capsaicin-induced intracellular Ca^{2+} influx through transient receptor potential V1 (TRPV1) channels. *J. Pharmacol. Sci.* **2016**, 130, 72-77.
22. Kallet, R.H.; Jasmer, R.M.; Luce, J.M.; Lin, L.H.; Marks, J.D. The treatment of acidosis in acute lung injury with tris-hydroxymethyl aminomethane (THAM). *Am. J. Respir. Crit. Care. Med.* **2000**, 161, 1149-1153.
23. Chen, X.; Wu, S.; Yi, M.; Ge, J.; Yin, G.; Li, X. Preparation and physicochemical properties of blend films of feather keratin and poly(vinyl alcohol) compatibilized by tris(hydroxymethyl)aminomethane. *Polymers* **2018**, 10, 1054.
24. Deacon, G.B.; Phillips, R.J. Relationships between the carbon-oxygen stretching frequencies of carboxylato complexes and the type of carboxylate coordination. *Coord. Chem. Rev.* **1980**, 33, 227-250.